I. Isasi et al., "A Multistage Algorithm for ECG Rhythm Analysis During Piston-Driven Mechanical Chest Compressions," in IEEE Transactions on Biomedical Engineering, vol. 66, no. 1, pp. 263-272, Jan. 2019, doi: 10.1109/TBME.2018.2827304..

A Multistage Algorithm for ECG Rhythm Analysis during Piston-Driven Mechanical Chest Compressions

Iraia Isasi, Unai Irusta*, *Member, IEEE* Elisabete Aramendi, Unai Ayala, Erik Alonso, Jo Kramer-Johansen, and Trygve Eftestøl, *Member, IEEE*

***Abstract*—*Goal:* An accurate rhythm analysis during cardiopulmonary resuscitation (CPR) would contribute to increase survival from out-of-hospital cardiac arrest. Piston-driven mechanical compression devices are frequently used to deliver CPR. The objective of this work was to design a method to accurately diagnose the rhythm during compressions delivered by a piston-driven device. *Methods:* Data was gathered from 230 out-of-hospital cardiac arrest patients treated with the LUCAS 2 mechanical CPR device. The dataset comprised 201 shockable and 844 nonshockable ECG segments, whereof 270 were asystole (AS) and 574 organized rhythm (OR). A multistage algorithm (MSA) was designed, which included two artifact filters based on a recursive least squares algorithm, a rhythm analysis algorithm from a commercial defibrillator, and an ECG-slope based rhythm classifier. Data was partitioned randomly and patient-wise into training (60%) and test (40%) for optimization and validation, and statistically meaningful results were obtained repeating the process 500 times. *Results:* The mean (standard deviation) sensitivity (SE) for shockable rhythms, specificity (SP) for nonshockable rhythms, and total accuracy of the MSA solution were: 91.7 (6.0), 98.1 (1.1) and 96.9 (0.9), respectively. The SP for AS and OR were 98.0 (1.7) and 98.1 (1.4), respectively. *Conclusions:* The SE/SP were above the 90/95% values recommended by the American Heart Association for shockable and nonshockable rhythms other than sinus rhythm, respectively. *Signi icance:* It is possible to accurately diagnose the rhythm during mechanical chest compressions and the results considerably improve those obtained by previous algorithms.**

***Index Terms*—Artifact suppression, cardiac arrest, cardiopulmonary resuscitation (CPR), electrocardiogram (ECG), mechanical chest compressions, piston-driven compressions, recursive least squares (RLS).**

Asterisk indicates corresponding author.

*U. Irusta is with the Department of Communications Engineering, University of the Basque Country UPV/EHU, Alameda Urquijo S/N, 48013 Bilbao, Spain (e-mail: unai.irusta@ehu.eus).

I. Isasi and E. Aramendi are with the Department of Communications Engineering, University of the Basque Country UPV/EHU, Alameda Urquijo S/N, 48013 Bilbao, Spain.

U. Ayala is with the Department of Signal Processing and Communications, Mondragon University, Loramendi, 4, 20500 Arrasate, Spain.

E. Alonso is with the Department of Applied Mathematics, University of the Basque Country UPV/EHU, Rafael Moreno Pitxitxi 3, 48013 Bilbao, Spain

J. Kramer-Johansen is with the Norwegian National Advisory Unit on Prehospital Emergency Medicine (NAKOS) and Department Of Anaesthesiology, Oslo University Hospital and University of Oslo, Pb 4956 Nydalen, 0424 Oslo, Norway.

T. Eftestøl is with the Department of Electrical Engineering and Computer Science, University of Stavanger, 4036 Stavanger, Norway.

I. INTRODUCTION

Early electrical defibrillation and high-quality chest compressions during cardiopulmonary resuscitation (CPR) are key for the outcome of out-of-hospital cardiac arrest patients [1]. Current treatment guidelines for cardiac arrest highlight the importance of minimizing interruptions in compressions during CPR [1]. However, for a reliable shock/no-shock decision, current defibrillators require interrupting compressions to avoid artifacts in the ECG. An accurate shock/no-shock decision during CPR would improve therapy in two ways. For nonshockable rhythms it would do away with unnecessary interruptions in CPR to check the rhythm. These interruptions, which compromise coronary perfusion pressure, worsen chest compression fraction and may result in decreased survival [2]. For ventricular fibrillation (VF) it would contribute to a quicker identification of the need to shock the patient, which is important given the high oxygen demands of VF [3].

Strategies to allow an accurate shock/no-shock decision without interrupting CPR therapy include analyzing the rhythm during pauses in compressions for ventilation, and using signal processing techniques to allow a reliable shock/no-shock decision during compressions. Pauses in compressions for ventilations occur approximately every 20 s in 30:2 CPR, and an accurate rhythm analysis during those pauses has already been demonstrated [4], [5]. However, those techniques are inapplicable to compression only CPR.

Solutions based on digital signal processing for a reliable shock/no-shock decision during compressions have followed two main approaches [6]: the design of adaptive filters to suppress the artifact followed by a defibrillator's shock/no-shock decision algorithm, and shock/no-shock decision algorithms based on robust ECG features minimally affected by the artifact. Adaptive filters address the spectral overlap between resuscitation cardiac rhythms and compression artifacts, and the time-varying spectral characteristics of the artifact. However, these filters require additional reference signals correlated to the artifact like compression force [7], thoracic impedance [8] or blood pressure [9]. Several solutions based on these signals have been developed including Wiener filters [10], recursive adaptive matching pursuit algorithms [11], [12] or Kalman state-space models [13]. Given the quasi-periodic nature of CPR artifacts, adaptive solutions to estimate a time-varying Fourier series model of the artifact have also been proposed, including Least Mean Squares (LMS) [14]–[16] or Kalman [17] solutions. Filtering schemes that use only the ECG to both characterize and remove the artifact include approaches based on coherent line removal [18], LMS [19] and Kalman filters [20].

Finally, two types of algorithms based on robust ECG-features have been proposed to classify the ECG during CPR: features computed without filtering like the morphological consistency algorithm [21], [22] and adaptive rhythm sequencing [23], or after filtering the artifact [24], [25]. Despite progress, current solutions do not allow a reliable rhythm analysis during CPR [6], either because filtering residuals may resemble VF in patients in asystole (AS), or because spiky residuals are interpreted as the QRS complexes of organized rhythms (OR) in patients in VF [15], [16].

In all of these studies artifacts originate from manual compressions delivered by rescuers. Mechanical compression devices are increasingly used in resuscitation although evidences of improved survival are not conclusive [26], [27], and have become popular in scenarios such as transportation, invasive-procedures or prolonged CPR [28]–[31]. Mechanical devices deliver compressions at a constant rate and depth in adherence with current resuscitation guidelines. There are two types of automated compressors available: pneumatically driven pistons like the LUCAS 2 (Physio-Control Inc/Jolife AB, Lund, Sweeden), and load distributing bands like the Auto Pulse (Zoll Circulation, Chelmsford, Massachusetts, USA) [32]. Preliminary attempts to remove the LUCAS 2 artifact with simple comb filters were promising on a limited dataset [33], even though filtering was later shown to be as challenging as for manual CPR artifacts when tested on a more comprehensive dataset [34]. Although mechanical CPR artifacts have a fixed frequency, they present larger amplitudes, significant filtering residuals, and many harmonics that make filtering the artifact challenging [34].

This study introduces a new method for a reliable shock/no-shock decision during piston-driven mechanical compressions. The approach uses two recursive least-squares (RLS) filters to reduce CPR artifacts, followed by three shock/no-shock decision stages based on a standard defibrillator algorithm and on an ECG-slope decision stage. The complete solution is therefore named multistage algorithm (MSA). The manuscript is organized as follows: Section II describes the study dataset; Section III introduces the time-varying Fourier series model of the artifact, an algorithm to estimate the order of the model, and the adaptive filter to track the time-varying Fourier coefficients; Section IV describes the building blocks and the general architecture of the MSA solution; Section V describes the performance metrics, data partition and optimization/test procedures; and the results, conclusions and discussion are presented in Sections VI to VIII.

II. Data Collection and Preparation

Data from 263 out-of-hospital cardiac arrest patients treated with the LUCAS 2 piston-driven chest compression device (Physio-Control Inc., Redmond, WA, USA) were reviewed. The cardiac arrest episodes were collected by the advanced life support responders of the emergency services of Oslo and Akershus (Norway) during 18 months in 2012 and 2013. Responders used Physio-Control's Lifepack 15 defibrillators that continuously record the ECG and impedance signals. The LUCAS 2 device delivers compressions in a fixed position, with constant depth (40-53 mm depending on chest height), at a constant rate ($102 \pm 2\,\mathrm{min}^{-1}$), with a 50% duty cycle, and allowing full chest recoil after each compression [35].

Anonymized data from the defibrillators was exported to Matlab (MathWorks Inc., Naick, MA) using Physio-Control's Code Stat data review software, and resampled to a sampling frequency of 250 Hz. The data included the ECG and impedance signals of each episode together with the compression instants detected by the Code Stat software.

The start of use of the LUCAS-2 device was marked when the compression rate stabilized at the device's fixed rate of $102\,\mathrm{min}^{-1}$ [34]. Then, 20 s signal segments with the same underlying rhythm were extracted during the device usage. The segments contained an initial 15 s interval during compressions to develop and evaluate our solution for the shock/no-shock decision during chest compressions, followed by a 5 s interval without compression artifacts to annotate the patient's rhythm. Fig. 1 shows two examples. Ground truth rhythm labels were adjudicated by consensus among two independent reviewers, a clinical researcher and a biomedical engineer, both specialized in resuscitation data science [34]. The rhythm annotators, who were not involved in the conception and development of the methods, examined the 5 s interval without artifacts (see Fig. 1) to annotate the rhythms. Segments were annotated as: VF and ventricular tachycardia (VT) in the shockable rhythm category, and OR and AS in the nonshockable category. Presence of pulse could not annotated because patient charts with clinical pulse annotations and/or capnography levels were not available. So the OR category includes both pulseless electrical activity and pulsed rhythms. Intermediate rhythms like fine VF (amplitude$<$200 μV) were discarded. The American Heart Association (AHA) does not establish a shock/no-shock recommendation for intermediate rhythms because the benefits of defibrillation are unclear for those rhythms [36].

The final annotated dataset consisted of 1045 segments from 230 patients, segments like the two examples shown in Fig. 1. There were 201 shockable segments (5 VT and 196 VF) from 62 patients, 270 AS segments from 99 patients and 574 OR segments from 160 patients. In what follows rhythms will be grouped into three categories: shockable (VF/VT), OR and AS. This is the typical rhythm class definition used in the literature on shock/no-shock decisions during CPR [15], [23]–[25]. The prevalence of VT in our dataset is low, although it is comparable to that of most similar studies [15], [16], [23], so a separate analysis for VT would not be meaningful.

III. Quasi-Periodic Model of the Artifact

A. Signal model

During chest compressions the ECG signal recorded by the defibrillator, $s_{\mathrm{cor}}(n)$, is corrupted by additive chest

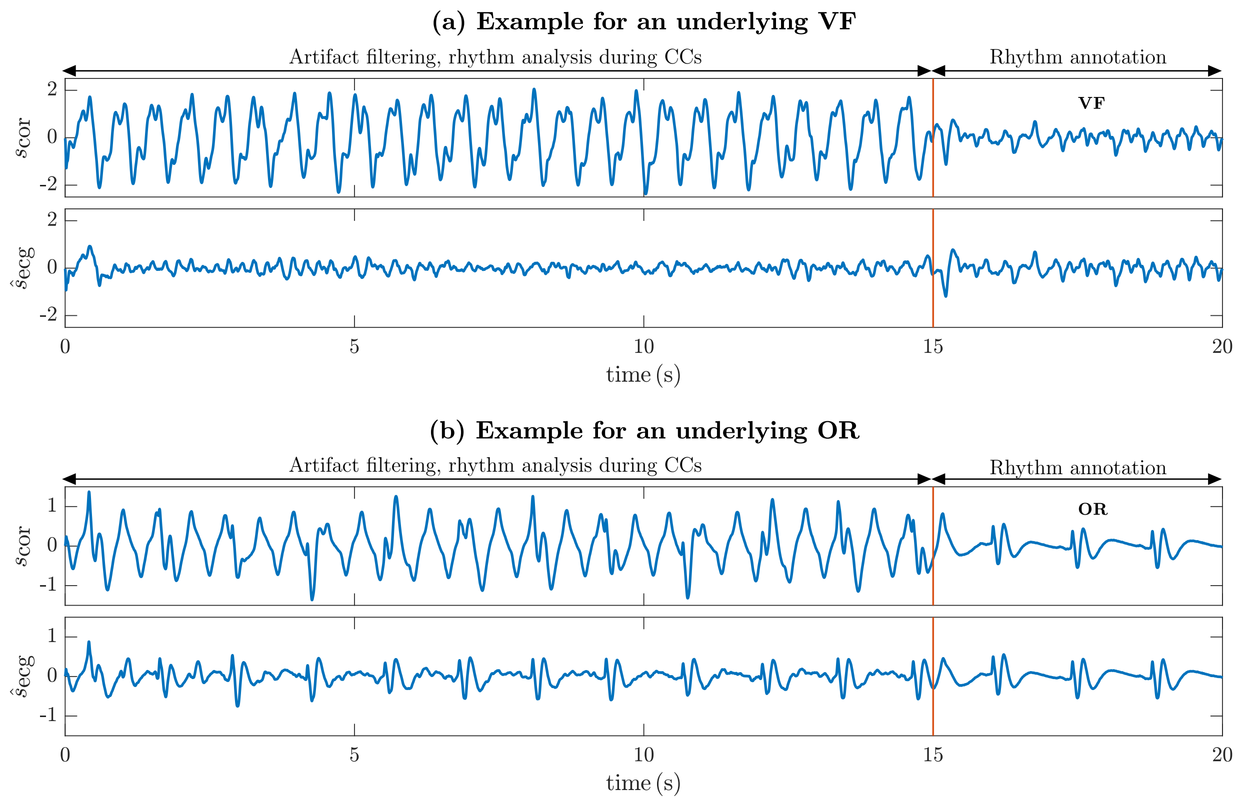

Fig. 1. Two examples of 20 s ECG segments corresponding to a patient in VF (example (a)) and to a patient in OR (example (b)). In both examples, the top panels show the ECG recorded by the device (the corrupt ECG, s_{cor}), and the bottom panels show the ECG after filtering the compression artifact (the estimated rhythm, $\hat{s}_{\text{ecg}}$). In the top panels, the initial 15 s of the ECG are corrupted by the LUCAS 2 artifact. The last 5 s show the underlying rhythm in an interval free of artifact. Filtering (bottom pannel in both examples) reveals the underlying rhythm.

compression artifacts, $s_{\text{cc}}(n)$, resulting in [11], [15]:

$$s_{\text{cor}}(n) = s_{\text{ecg}}(n) + s_{\text{cc}}(n) \tag{1}$$

where $s_{\text{ecg}}(n)$ is the patient's clean ECG reflecting the actual underlying heart rhythm. Methods focus on estimating the artifact $s_{\text{cc}}(n)$. An extensively used approach is to assume $s_{\text{cc}}(n)$ to be quasi-periodic and thus model the artifact as a truncated Fourier series of N terms [14]–[16] with no DC-component. The Fourier series can be expressed in terms of the amplitude and phase coefficients, $c_k(n)$ and $\theta_k(n)$, or as a sine-cosine series with in-phase and cuadrature amplitudes, $a_k(n)$ and $b_k(n)$, in the following way:

$$s_{\text{cc}}(n) = A(n) \sum_{k=1}^{N} c_k(n) \cos(k\omega_0 n + \theta_k(n)) = \tag{2}$$

$$= A(n) \sum_{k=1}^{N} \big(a_k(n) \cos(k\omega_0 n) + b_k(n) \sin(k\omega_0 n) \big) \tag{3}$$

where $A(n)$ is an amplitude term to model intervals with compressions, $A(n) = 1$, and without compressions, $A(n) = 0$, such as hands-off intervals for ventilations. Smooth transitions between intervals were defined as described in [15], [37]. The spectral components of the artifact, its Fourier coefficients, are considered time-varying and will be tracked using an adaptive RLS filter (see subection III-C). The frequency ω_0 is the fundamental discrete frequency of the compressions which for a piston-driven compression device is constant:

$$\omega_0 = 2\pi f_{\text{LUCAS}} T_s \tag{4}$$

with $f_{\text{LUCAS}} = 1.694\,\text{Hz} \equiv 101.6\,\text{min}^{-1}$ [34], and T_s the sampling period.

B. Estimating the number of harmonics N

Previous works have assumed the number of harmonics N to be fixed for all cases. However, the spectral content of the artifact is very variable from case to case both in manual [15] and mechanical compressions [34], and depends on factors like the rescuer, the patient or electrode placement. Estimating N in manual CPR is unfeasible or inaccurate because compression frequency changes with every compression. In mechanical CPR the frequency is fixed and simple spectral methods can be used to estimate the number of significant coefficients in (2). Assuming constant c_k coefficients, which suffices for approximate power computations but not for rhythm analysis, we can express the power of the artifact in short ECG intervals using Parseval's theorem:

$$P_{\text{cc}} \approx \sum_{k=1}^{N} c_k^2 = \sum_{k=1}^{N} \left(a_k^2 + b_k^2 \right) \tag{5}$$

In this work we determined the number of significant harmonics as the first integer $N \leq 30$ for which the following inequality holds:

$$100 \cdot \frac{P_{\text{cc},N+3} - P_{\text{cc},N}}{P_{\text{cc},N}} \leq \gamma \quad \text{with} \quad P_{\text{cc},K} = \sum_{k=1}^{K} c_k^2 \tag{6}$$

i.e. when the addition of 3 new harmonics increased the relative power by less than the threshold γ, optimized in the simulation phase. The problem then reduces to efficiently estimating the amplitudes c_k located at fixed frequencies $k\omega_0$.

The Fourier coefficients were estimated using the Generalized Goertzel Algorithm. The standard Goertzel algorithm allows the direct evaluation of isolated terms of the discrete Fourier transform. Its generalization extends the method to compute spectral components at any frequency [38], in our case the $k\omega_0$ frequencies. Therefore, $X(k\omega_0)$, the spectral components of the signal $x(n)$ at our frequencies of interest were computed using the following equations [38]:

$$s(n) = x(n) + 2\cos(k\omega_0)s(n-1) - s(n-2) \tag{7}$$

$$X(k\omega_0) = \left(s(L_g) - e^{-jk\omega_0}s(L_g-1)\right)e^{-jk\omega_0 L_g} \tag{8}$$

where L_g is the length of the signal $x(n)$. For mechanical chest compression artifacts we assume that the ECG components at $k\omega_0$ are negligible when compared to the harmonics of the artifact, and therefore $x(n) = s_{\text{cor}}(n)$. We used the initial 5 s window ($L_g = 5 \cdot f_s$) with compressions to estimate the c_k, and formed a windowed signal $x_w(n) = s_{\text{cor}}(n) \cdot w_\beta(n)$, where $w_\beta(n)$ is a Kaiser window with form factor $\beta = 4.5$ to reduce spectral leakage. The c_k coefficients were obtained as:

$$c_k = |X(k\omega_0)| = \left| \frac{2}{W_{4.5}(0)} X_w(k\omega_0) \right| \tag{9}$$

Here $W_{4.5}(0)$ is the spectral component of the Kaiser window at the origin, and $X_w(k\omega_0)$ are the spectral components of $x_w(n)$ at the harmonic frequencies.

C. Estimation of the $a_k(n)$ and $b_k(n)$ coefficients

Constant Fourier coefficients were assumed to determine N, the order of the model for each case. However, a proper rhythm analysis requires tracking the time-varying characteristics of the spectral components of the artifact, the coefficients in (3). These were estimated using an RLS Fourier analyzer [39], adapted to estimate mechanical CPR artifacts [40]. The RLS filter presents improved convergence and adaptability characteristics when compared to the LMS approach formerly used for CPR artifact suppression [14]–[16]. First we define two vectors for the coefficients and reference signals (the harmonic components):

$$\mathbf{\Theta}(n) = [a_1(n)\, b_1(n)\, \ldots\, a_N(n)\, b_N(n)]^T \tag{10}$$

$$\mathbf{\Phi}(n) = [\cos(\omega_0 n)\ \sin(\omega_0 n)\ \ldots\ \cos(N\omega_0 n)\ \sin(N\omega_0 n)]^T \tag{11}$$

Then the estimated chest compression artifact, $\hat{s}_{\text{cc}}(n)$, is:

$$\hat{s}_{\text{cc}}(n) = A(n)\mathbf{\Theta}^{\mathbf{T}}(n-1)\mathbf{\Phi}(n) \tag{12}$$

Filter coefficients are updated using the RLS algorithm to minimize the error between the corrupt ECG and the estimated artifact at the harmonics of the mechanical chest compression frequency. The error signal is the ECG of the estimated underlying rhythm, $\hat{s}_{\text{ecg}}$, and the update equations are:

$$\hat{s}_{\text{ecg}}(n) = s_{\text{cor}}(n) - \hat{s}_{\text{cc}}(n) \tag{13}$$

$$\mathbf{F}(n) = \frac{1}{\lambda}\left[\mathbf{F}(n-1) - \frac{\mathbf{F}(n-1)\mathbf{\Phi}(n)\mathbf{\Phi}^T(n)\mathbf{F}(n-1)}{\lambda + \mathbf{\Phi}^T(n)\mathbf{F}(n-1)\mathbf{\Phi}(n)}\right] \tag{14}$$

$$\mathbf{\Theta}(n) = \mathbf{\Theta}(n-1) + \mathbf{F}(n)\mathbf{\Phi}(n)\hat{s}_{\text{ecg}}(n) \tag{15}$$

where the gain matrix and coefficient vector were initialized to $\mathbf{F}(0) = 0.03\mathbf{I}_{2N}$ and $\mathbf{\Theta}(0) = \mathbf{0}^T$. The forgetting factor of the RLS algorithm, λ, governs the performance of the filter and is set very close to unity. The choice of the forgetting factor is a compromise between the tracking capabilities and misadjustment and stability. Forgetting factors very close to unity ($\lambda > 0.995$) mean low misadjustments and good stability, but reduced tracking capabilities. This is desirable when the underlying rhythm (error signal) presents abrupt changes like QRS complexes, for instance in some OR rhythms. Smaller values of λ ($0.980 < \lambda < 0.995$) produce fast tracking capabilities but larger misadjustements and poorer stability. This may be desirable when the underlying rhythm is negligible, such as during AS. The different qualitative behaviors of the filter will be exploited by the MSA solution that uses two configurations of the RLS filter, as described in the following section.

IV. ARCHITECTURE OF THE SOLUTION

A. Rhythm analysis

Filtering should reveal the underlying heart rhythm of the patient, consequently $\hat{s}_{\text{ecg}}(n)$ was used to diagnose the rhythm as shockable or nonshockable. Two different approaches were used to diagnose the rhythm: an AHA compliant rhythm analysis algorithm designed to diagnose clean ECG, and an ECG feature designed to discriminate OR and VF rhythms after filtering the CPR artifact.

The rhythm analysis algorithm used was originally designed to diagnose artifact-free ECG, and uses 3 consecutive ECG intervals of 3.2 s to give a shock/no-shock decision. Succinctly, for an in depth description consult chapter 4 (pages 63-111) of [41], the decision is performed in three different stages. The first one discriminates asystole segments by identifying the absence of electrical activity based on the amplitude and power of the ECG. In the second stage, three parameters that identify the presence of QRS complexes are fed in a binary classifier based on a multiple logistic regression model to discriminate OR and shockable rhythms [42]. Finally a patch is added to discriminate fast ventricular from supraventricular rhythms [43]. The code for the computations of the features is avaliable through [44]. The algorithm was developed and tested following AHA recommendations for arrhythmia analysis algorithms in defibrillators [36], and is fully AHA compliant [41], [42]. Furthermore, it is currently in use in the Reanibex R-series defibrillator (Bexen Cardio S. Coop., Ermua, Spain).

The algorithm was designed to diagnose artifact-free ECG, and uses 9.6 s ECG intervals to give a shock/no-shock decision. In this work we fed the rhythm analysis algorithm with a 9.6 s interval of the filtered ECG (from 3.4 s to 13 s), the first 3.4 s were left out to avoid RLS filter transients.

The OR/VF discrimination feature is based on the slope of the filtered ECG [25], and was computed using the same signal interval of $\hat{s}_{\text{ecg}}(n)$ fed to the rhythm analysis algorithm (from 3.4 s to 13 s). The slope was obtained as the first difference, it was then squared and passed through a moving average filter of M samples (80 ms) and normalized by its maximum value, to obtain:

$$d(n) = \frac{1}{M}\sum_{m=0}^{M-1}(\hat{s}_{\text{ecg}}(n-m) - \hat{s}_{\text{ecg}}(n-m-1))^2 \tag{16}$$

$$\overline{d(n)} = \frac{d(n)}{\max\{d(n)\}} \quad n = 0, ..., L_a - 2 \tag{17}$$

where $L_a = 9.6 \cdot f_s$ is the length in samples of the interval. The discrimination feature is called slope baseline (bS) [25] and was obtained as the 10$^{\text{th}}$ percentile of $\overline{d(n)}$ in the analysis interval. OR rhythms present large slopes only around QRS complexes leading to low values of bS. In contrast, VF rhythms present evenly distributed slopes, thus larger values of bS. The averaging filter contributes to eliminate the effect of filtering residuals [25].

B. Architecture of the MSA solution

The general architecture of the MSA solution for the shock/no-shock decision during mechanical chest compressions is shown in Fig. 2, and is composed of three stages. The process starts by determining the number of significant harmonics of the artifact using the generalized Goertzel method (section III-B). In stage 1, the corrupt ECG is coarsely filtered using the RLS filter with a $\lambda_1 \sim 0.990$, to identify AS segments. If the rhythm analysis algorithm identifies a nonshockable rhythm the process ends, otherwise stage 2 is activated. In stage 2, the corrupt ECG is finely filtered using the RLS filter with a $\lambda_2 \sim 0.999$, in order to preserve quick ECG variations like QRS complexes. Again if the algorithm identifies a nonshockable rhythm the process ends, otherwise stage 3 is activated. In stage 3, the finely filtered ECG is used to compute bS and discriminate OR from VF. Four free parameters were left to optimize the performance of the solution: the threshold to determine the order of the CPR artifact model (γ), the forgetting factors of the filters (λ_1 and λ_2), and the bS threshold (ρ).

V. EVALUATION AND OPTIMIZATION

The performance of the method was evaluated by comparing the shock/no-shock decisions of our method for the filtered intervals with the clinicians' rhythm annotations for the artifact-free intervals. The following metrics were

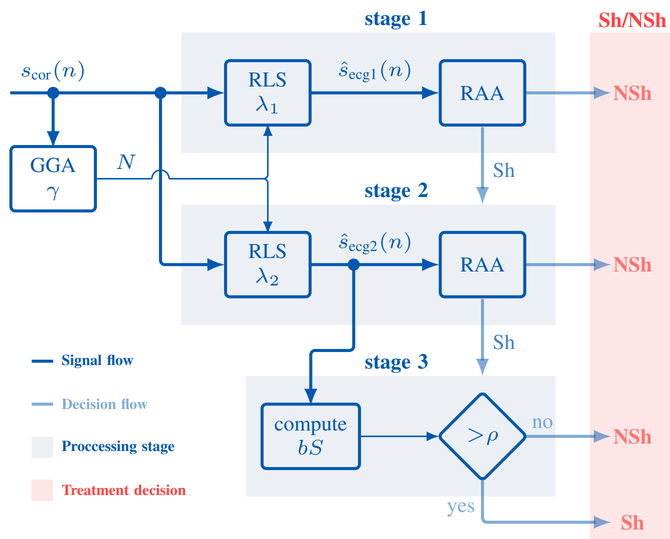

Fig. 2. Architecture of the MSA solution for shock (Sh) and no-shock (NSh) decisions during mechanical compressions. The solution is composed of three analysis stages: a first stage based on a coarse RLS adaptive filter ($\lambda_1 \sim 0.99$), a second stage with a fine RLS filter ($\lambda_2 \sim 0.999$) and a third stage based on the slope analysis (bS) of the filtered ECG. In stages 1 and 2 the decision is based on an AHA commpliant rhythm analysis algorithm (RAA). The order N of the RLS filters is determined using the Generalized Goertzel Algorithm (GGA). The stages are activated sequentially and the process ends when a no-shock decision is reached in stages 1 or 2, or with any diagnosis at stage 3.

computed: sensitivity (SE), the proportion of correctly identified shockable segments; specificity (SP), the proportion of correctly identified nonshockable segments; accuracy (Acc), the proportion of correct decisions; and balanced accuracy (BAC). The BAC is the mean value of SE and SP,

$$\text{BAC} = \tfrac{1}{2}(\text{SE} + \text{SP}) \tag{18}$$

and gives an unbiased measure of the method's perfomance which is desirable during optimization given the different prevalences of shockable and nonshockable segments in our dataset. BAC can be interpreted as a particular case of the unbiased mean of sensitivities for multiclass problems [45].

Data was partitioned patient-wise, 60% of patients were included in the training dataset to optimize the values of γ, λ_1, λ_2, and ρ, and 40% of patients were left for testing to compute SE, SP, BAC and Acc. Since the partition of the data can have a significant impact on the results, the process was repeated for 500 random 60/40 patient-wise partitions to obtain statistically meaningful results. We used 500 bootstrap replicas because in our preliminary experiments a number of replicas above 300 ensured the repeatability and reliability of the estimates of the statistical distributions of the performance metrics. These distributions of the performance metrics were tested for normality using the Kolmogorov-Smirnov test, and were reported as mean value and standard deviation since they followed normal distributions.

For each of the 500 partitions the optimization process comprised three steps. First, the pair (γ, λ_1) that maximized the BAC for stage 1 of the training set was determined by doing a greedy search in the $0 < \gamma < 0.07$ and $0.985 <$

$\lambda < 0.995$ ranges. Second, the value λ_2 that maximized the SP for OR in stage 2 was determined by searching the $0.9950 < \lambda < 0.9999$ range. Third, two values of ρ were determined using the training segments that made it to stage 3. The first (ρ_1) and second (ρ_2) values set the threshold of correctly detected VF segments at 99% (high SE) and 95% (high SP), respectively.

The results were compared to those obtained for the filtering methods proposed in the literature to suppress chest compression artifacts from piston-driven devices: the LMS filter [15], [34] and the comb filter [33], [34]. For a fair comparative assessment, the training/test procedure used for the RLS was replicated. Therefore, the filters were optimized as in stage 1 of the solution proposed in this paper, that is by adjusting (γ, BW) in the comb filter and (γ, μ) in the LMS filter. In the comb filter BW refers to the bandwidth around each notch (multi-notch filter), and for the LMS filter μ is the step size of the LMS algorithm. The algorithmic details can be found in the original references [15], [33], [34].

VI. RESULTS

The dependence of the order of the model, i.e. the number of harmonics N, with the power threshold γ is shown in Fig. 3. For small values of the threshold, $\gamma < 0.005$, the median model order is above 20 but the variability is large. For instance, for $\gamma = 0.005$ model orders ranged from 8–30, and in 90% of cases were in the 11–27 range. This indicates that although many harmonics are required to accurately represent the piston-driven chest compression artifact ($N > 15$), the variability is large from case to case, and that it is important to adjust the order of the model in the prefiltering stage. Furthermore, Fig. 3 shows differences in model order depending on the underlying rhythm. Nonshockable rhythms (AS and OR) presented larger orders than shockable rhythms, because in the latter Goertzel's coefficient estimation may be affected by the spectral overlap of the underlying rhythm and the artifact.

Fig. 4 shows filtering examples for the three rhythm types, and the two filter configurations, coarse ($\lambda_1 = 0.990$) and fine filtering ($\lambda_2 = 0.999$). Both filter configurations reveal the underlying VF equally well in the example in panel (a). For nonshockable rhythms, coarse filtering has a larger negative effect on signal amplitude in OR rhythms, as shown by the lower amplitude of the QRS complexes in the example of panel (b). However, fine filtering leaves a larger filtering residual than can mislead rhythm analysis during AS, as shown in the example of panel (c). So a compromise between both filtering characteristics is needed for an accurate rhythm analysis. For a better understanding of the filter characteristics (λ_1/λ_2) with OR rhythm the reader can consult the additional filtering examples in the supplementary materials, which also provide additional filtering experiments that explain the differences observed for OR rhythms for the two filter configurations.

The effectiveness of the RLS filter is summarized in Fig. 5, which shows the SE, SP and BAC of the rhythm analysis algorithm after filtering the chest compression artifact. This is equivalent to using only stage 1 in the filtering solution. The figure shows four implementations of the filter: for a fixed order ($N = 30$, $\gamma = 0$), and for three case dependent orders, with a small threshold ($\gamma = 0.002$, i.e. large N), intermediate treshold ($\gamma = 0.070$, i.e. intermediate N) and large threshold ($\gamma = 0.400$, i.e. small N). In addition the filter's optimal working range in the BAC sense is highlighted. The best results were obtained for small γ, and the figure shows that a case dependent order was particularly important to improve SP, which is where CPR suppression filters are known to fail [6].

The performance metrics for the 500 random patient-wise training/test partitions are shown in Table I. All metrics are reported as mean (standard deviation). Metrics were computed for different configurations of the filtering solution including only one, two or all three stages described in Fig. 2. The results are compared to the single stage LMS and comb filters proposed in the literature, and to the results obtained for the unfiltered ECG. Filtering increased the BAC by over 20-points in all cases. The RLS filter was the best single stage method, its BAC was 1.2-points above that of the LMS filter. Furthermore the addition of stages 2 and 3 increased the overall BAC by around 3-points and most importantly the SP by over 8-points. Stage 3 allows a trade-off between the SE and SP of the solution. The 3-stage MSA solution produced SE/SP pairs above the minimum 90/95 values recommended by the AHA [36] for rhythm analysis on clean ECGs. As in previous works on shock/no-shock decision during manual CPR, the performance goal for nonshockable rhythms was fixed at 95 % specificity [9], [14]–[16], [24]. This is the AHA performance goal for asystole and for rhythms other than normal sinus rhythm. For safety reasons, the AHA recommends a 99 % specificity for normal sinus rhythms. However, organized rhythms during cardiac arrest are rarely normal sinus rhythms, since restoration of a normal rhythm and pulse would imply ceasing chest compression therapy.

The average characteristics of the optimal MSA solution

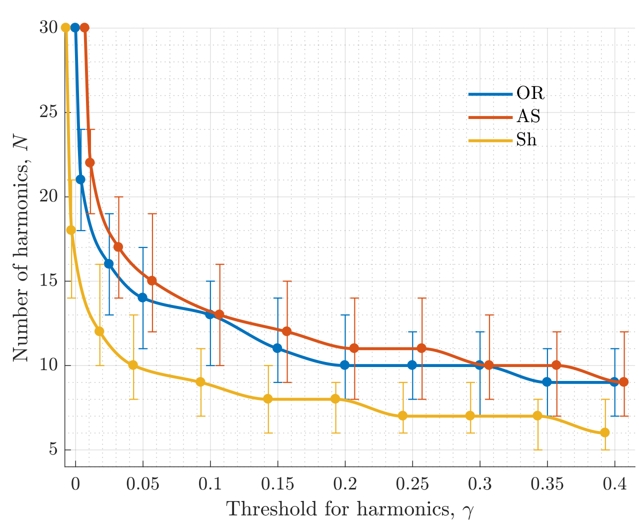

Fig. 3. Distribution of the number of harmonics as a function of the harmonic selection threshold (γ). The graph shows the median value and the 25-75 percentile range for the complete dataset. Data is shown for all cases differentiated by rhythm type: OR, AS and shockable.

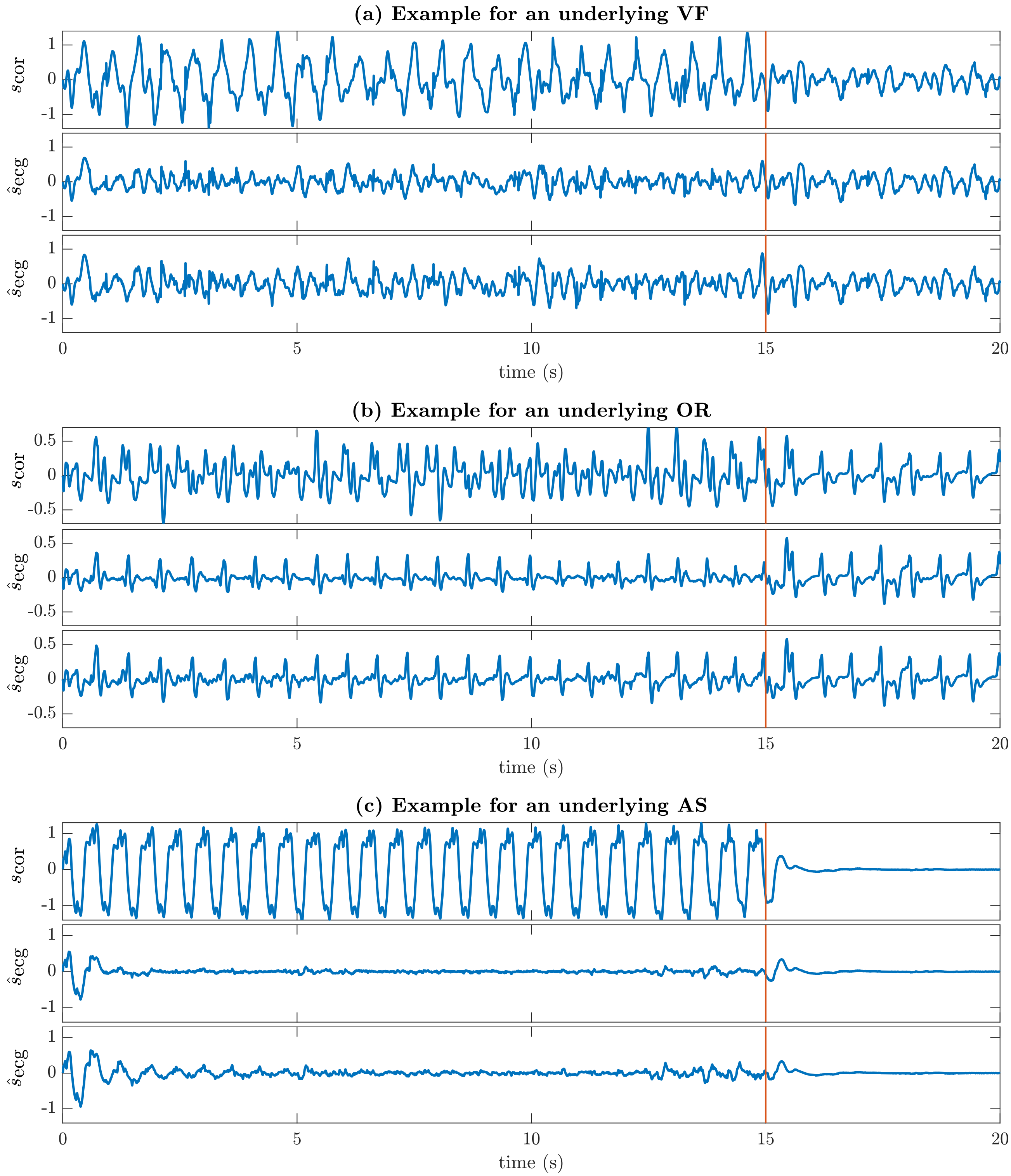

Fig. 4. An example of unfiltered and filtered AS (a), OR (b) and VF (c) rhythms. The first graph of each panel shows the unfiltered ECG, whereas the other two show the filtered ECG for both filtering stages, coarse filtering ($\lambda_1 = 0.990$) in the middle and fine filtering ($\lambda_2 = 0.999$) in the bottom graphs.

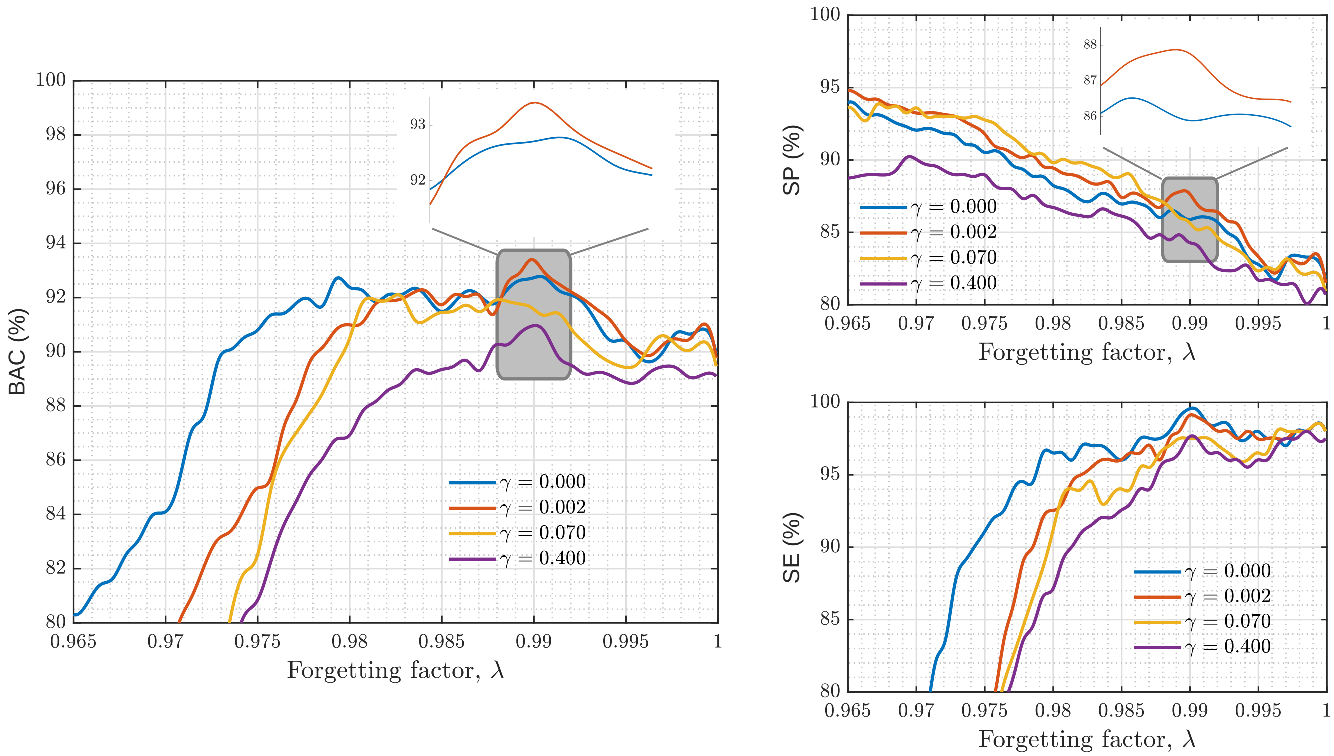

Fig. 5. Performance metrics for a single stage RLS filter. Data was obtained for the whole dataset and is shown as a function of the forgetting factor of the filter (λ) for four thresholds: $\gamma = 0$ ($N = 30$ fixed), $\gamma = 0.002$ (large N), $\gamma = 0.07$ (intermediate N) and $\gamma = 0.4$ (small N). The highlighted region shows the optimal range of the filter in the BAC sense, and shows that the best results were obtained for small γ (red).

were $\lambda_1 = 0.9899\,(0.0006)$, $\gamma = 2.3\,(1.3) \cdot 10^{-3}$, $\lambda_2 = 0.9990\,(0.0003)$, $\rho_1 = 7.7\,(4.3) \cdot 10^{-3}$ and $\rho_2 = 16.7\,(4.4) \cdot 10^{-3}$. On average 70.7% of segments were diagnosed in stage 1, 5.4% in stage 2 and 23.9% in stage 3. The drawback of an RLS based solution is the processing time, and in particular the recursion formula for the gain matrix which involves the multiplication of $2N \times 2N$ matrices (equation (14)). Our Matlab implementation of the RLS filter (single stage) on an i7 3.2 GHz single-core processor and 16 GB of memory took on average 85 ms, considerably more than the 17 ms and 8 ms obtained for the LMS and the comb filters, respectively. The computational demands of the RLS filter are acceptable for the implementation on current monitor/defibrillators, but processing demands could be reduced by an order of magnitude using an MSA solution based on the comb filter, of five-fold using the LMS filter.We implemented those solutions, by replicating the optimization process used for the RLS filter and using for stage 2 a bandwidth range of $0.08 < BW < 0.2$ Hz for the comb filter, and a step size range of $0.0009 < \mu < 0.002$ for the LMS filter, which are equivalent to the range of large forgetting factors in the RLS filter. Table II compares the MSA solutions based on the RLS, LMS and comb filters, and shows there is a trade-off between diagnostic accuracy and computational demands. The table also shows the classification per rhythm type, to describe the effect of each stage of the MSA solution on the accuracy for each rhythm type. In fact, the AHA's requirements for all rhythm types were only met by the 3-stage RLS based solutions.

VII. DISCUSSION

This paper introduces a MSA solution for an accurate shock/no-shock decision during mechanical CPR. The solution introduces and/or combines several features that contribute to an increased decision accuracy: an improved CPR artifact filter with a per case filter order (genelarized Goertzel algorithm) and better tracking characteristics (RLS filter), a two-stage filtering approach to improve SP, and a final VF/OR discrimination algorithm to balance the SE and SP of the solution. It improves the BAC, SP and Acc of previous solutions by more than 5-points, 12-points and 10-points, respectively. The MSA is the first solution to meet AHA's criteria for SE/SP during mechanical compressions, with a specificity above the 95 % AHA recommendation for nonshockable rhythms other than sinus rhythm.

Mechanical compressions are delivered at a fixed frequency, this allowed the realization of a simple and computationally efficient method to determine the order of the model. Previous attempts to remove the LUCAS 2 artifact focused on the identification of an overall optimal model order [33], [34], but our results show that model orders vary considerably from case to case and that a case dependent order contributes to an improved SP. RLS Fourier analyzers present improved convergence, shorter transients and better tracking properties [39] than the previously used LMS [14], [15], [19] or Kalman filters [17]. The RLS filter improved the BAC of the LMS filter by 1.2-points, and the effect was larger on the SP (see table I). The last two characteristics of the MSA solution were inspired by two recent solutions to allow accurate shock/no-shock decisions during manual CPR. Iterative artifact filtering was introduced within the enhanced adaptive filter (EAF) [16]. In our case, two filtering stages were sufficient, a coarse filter to maximize BAC (stage 1) and a fine filter to improve the detection of OR rhythms (stage 2). The analysis of the slope, an approach introduced by Ayala *et al.* [25] to classify the filtered ECG, improved the SP of our method by 2-4 points depending on the configuration of the detection threshold. These two additions boosted the SP above 95% and were particularly important to increase SP for OR rhythms by 10 to 14-points (see table II).

Mechanical chest compression devices are popular in emergency services. Data from a US cardiac arrest registry indicated that 45% of participating services routinely used mechanical devices [46]. Current resuscitation guidelines for instance recommend their use in situations where sustained high quality manual chest compressions are impractical or unsafe [32]. It is therefore important to devise methods to reduce the compression artifact and allow an accurate shock/no-shock decision during therapy. When compared to filtering manual compression artifacts, mechanical compression artifacts present advantages and challenges. Mechanical artifact filtering is easier because the compression frequency is fixed and the artifact waveform pattern more stable [34]. Challenges include larger artifact amplitudes [33], [34], and larger harmonic content, producing models with very large orders and increased computational cost.

Many CPR artifact filters for manual chest compressions have used additional reference signals to model the artifact [7], [9], [11]–[13], [16]. The acquisition of signals like compression depth, acceleration or force makes defibrillator hardware more complex and expensive, so these reference signals are not universally available [6]. Irusta et al showed that chest compression rate derived from the depth signal was sufficient to accurately model the artifact [15]. In fact, when compared on the same data and with the same shock/no-shock decision algorithm, adaptive filters based only on chest compression rate were as accurate as adaptive filters using four reference channels [47]. Piston-driven mechanical chest compressions are delivered at a fixed frequency, so the problem is further simplified because depth or impedance are no longer needed to determine the chest compression rate. Furthermore, for manual CPR computing chest compression rate from signals like impedance, depth or force requires algorithms that accurately identify compression related fiducial points (maximum depth). These fiducial points cannot be always accurately determined, and this negatively affects the performance of the adaptive solutions based only on rate [14]. Our simulations for the MSA method on manual CPR data (see Section I of the supplementary materials) confirm this hypothesis. Artifact filtering during manual CPR based only on the ECG involves an additional stage to determine compression frequency for which methods using spectral analysis [20], [48], empirical mode decomposition [19], or coherent line removal [18] have been devised. Some of these methods could be adapted in the future to implement a prefiltering stage to determine a case dependent model for manual CPR artifacts. Increasing the SP of shock/no-shock decisions during manual chest compressions remains a challenge but future solutions should probably include multistage filters and post-filtering stages such as spiky artifact detectors [16] and ad-hoc solutions to discriminate rhythms based on the filtered ECG [21], [24], [25].

This study has some limitations. First, the MSA method is computationally demanding. The filtering stages could be simplified using computationally efficient RLS Fourier analyzers [39], LMS filters, or comb filters, but the cost would be a lower accuracy. Second, compressions were delivered using a piston-driven device, and artifact characteristics may differ when load distribution bands are used. Third, data were gathered using only one monitor/defibrillator model and extrapolation of the results to other models may involve adjusting the method for different sampling frequencies, voltage resolutions and ECG acquisition bandwidth. And fourth, data was gathered from a single emergency service, and there may be differences in resuscitation protocols and device usage across services [46] that may alter the characteristics of the CPR artifacts.

TABLE I
PERFORMANCE OF THE MSA SOLUTION PRESENTED STEP-WISE AND COMPARED TO PREVIOUS PROPOSALS BASED ON LMS AND COMB FILTERS.

Method	SE (%)	SP (%)	BAC (%)	Acc (%)
Before filtering	50.7	83.9	67.3	77.5
MSA solution				
stage 1	98.1 (1.0)	87.0 (1.8)	92.5 (1.1)	89.1 (1.5)
stage 2	97.4 (2.0)	93.5 (1.2)	95.5 (1.0)	94.3 (1.0)
stage 3 (high SE)	95.0 (4.0)	95.4 (1.8)	**95.2** (1.4)	95.3 (1.1)
stage 3 (high SP)	91.7 (6.0)	**98.1** (1.1)	94.9 (2.6)	**96.9** (0.9)
LMS [34]	98.6 (1.0)	84.0 (1.8)	91.3 (1.2)	86.8 (1.6)
Comb [33], [34]	97.1 (2.0)	84.3 (1.8)	90.7 (1.3)	86.8 (1.6)

TABLE II
COMPARISON BETWEEN MSA SOLUTION BASED ON RLS, LMS AND COMB FILTERS, INCLUDING PROCESSING TIMES.

MSA solution	SE (%)	SP (%)		ptime (ms)
		AS	OR	
RLS based				
stage 1	98.1 (1.0)	93.0 (2.7)	84.2 (2.2)	85
stage 2	97.4 (2.0)	95.3 (2.2)	92.7 (1.5)	110
stage 3 (high SE)	95.0 (4.0)	96.3 (2.3)	95.0 (2.1)	111
stage 3 (high SP)	91.7 (6.0)	98.0 (1.7)	98.1 (1.4)	111
LMS based				
stage 1	98.6 (1.0)	87.7 (3.1)	82.3 (2.3)	16
stage 2	96.0 (2.0)	94.2 (2.3)	92.0 (1.6)	21
stage 3 (high SE)	94.4 (3.0)	95.0 (2.3)	92.3 (1.6)	21
stage 3 (high SP)	90.4 (5.0)	95.3 (2.2)	92.4 (1.5)	21
COMB based				
stage 1	97.1 (2.0)	86.7 (4.1)	83.2 (2.6)	8
stage 2	94.6 (2.0)	91.2 (3.4)	89.3 (2.1)	11
stage 3 (high SE)	92.4 (4.0)	93.6 (2.7)	93.1 (2.7)	11
stage 3 (high SP)	88.8 (6.0)	95.9 (2.4)	96.9 (1.7)	11

VIII. CONCLUSIONS

This paper introduces the first method to give a shock/no-shock diagnosis compliant with AHA recommendations for shockable (SE above 90%) and nonshockable rhythms (SP above 95% for rhythms other than sinus rhythm) during mechanical chest compressions. The MSA method had an SE of 91.8% and an SP of 98.1%, for an accuracy of 96.9%. A two stage filtering approach combined with an ad-hoc algorithm to differentiate OR from VF were implemented to increase the SP, which was well below 90% in all previous studies. This new approach to rhythm diagnosis during chest compressions may open the possibility of diagnosing the rhythm without interrupting compression therapy.

IX. ACKNOWLEDGMENT

This work received financial support from the Spanish Ministerio de Economía y Competitividad, project TEC2015-64678-R jointly with the Fondo Europeo de Desarrollo Regional (FEDER); from UPV/EHU via project UPV/EHU 16/18, and from the Basque Government through grant PRE-2016-1-0012. The authors would like to thank the patients and the EMS-providers for their contribution with valuable data, and H Naas for his help on the preparation of the data. The authors would like to thank the anonymous reviewers for their insightful critique and suggestions for further experiments which have increased the relevance and scope of the work.

REFERENCES

[1] G. Perkins, A. Handley, R. Koster, M. Castrén, M. Smyth, T. Olasveengen, K. Monsieurs, V. Raffay, J. Gärsner, V. Wenzel *et al.*, "European resuscitation council guidelines for resuscitation 2015: Section 2. adult basic life support and automated external defibrillation," *Resuscitation*, vol. 95, no. Oct, pp. 81–99, 2015.

[2] C. Vaillancourt, S. Everson-Stewart, J. Christenson, D. Andrusiek, J. Powell, G. Nichol, S. Cheskes, T. P. Aufderheide, R. Berg, I. G. Stiell *et al.*, "The impact of increased chest compression fraction on return of spontaneous circulation for out-of-hospital cardiac arrest patients not in ventricular fibrillation," *Resuscitation*, vol. 82, no. 12, pp. 1501–1507, 2011.

[3] M. G. Hoogendijk, C. A. Schumacher, C. N. Belterman, B. J. Boukens, J. Berdowski, J. M. de Bakker, R. W. Koster, and R. Coronel, "Ventricular fibrillation hampers the restoration of creatine-phosphate levels during simulated cardiopulmonary resuscitations," *Europace*, vol. 14, no. 10, pp. 1518–1523, 2012.

[4] J. Ruiz, U. Ayala, S. R. de Gauna, U. Irusta, D. González-Otero, E. Alonso, J. Kramer-Johansen, and T. Eftestøl, "Feasibility of automated rhythm assessment in chest compression pauses during cardiopulmonary resuscitation," *Resuscitation*, vol. 84, no. 9, pp. 1223–1228, 2013.

[5] U. Ayala, U. Irusta, J. Ruiz, S. R. de Gauna, D. González-Otero, E. Alonso, J. Kramer-Johansen, H. Naas, and T. Eftestøl, "Fully automatic rhythm analysis during chest compression pauses," *Resuscitation*, vol. 89, pp. 25–30, 2015.

[6] S. Ruiz de Gauna, U. Irusta, J. Ruiz, U. Ayala, E. Aramendi, and T. Eftestøl, "Rhythm analysis during cardiopulmonary resuscitation: past, present, and future," *BioMed research international*, vol. 2014, 2014.

[7] R. D. Berger, J. Palazzolo, and H. Halperin, "Rhythm discrimination during uninterrupted CPR using motion artifact reduction system," *Resuscitation*, vol. 75, no. 1, pp. 145–152, 2007.

[8] S. Babaeizadeh, R. Firoozabadi, C. Han, and E. D. Helfenbein, "Analyzing cardiac rhythm in the presence of chest compression artifact for automated shock advisory," *Journal of electrocardiology*, vol. 47, no. 6, pp. 798–803, 2014.

[9] T. Werther, A. Klotz, G. Kracher, M. Baubin, H. G. Feichtinger, H. Gilly, A. Amann *et al.*, "CPR artifact removal in ventricular fibrillation ECG signals using Gabor multipliers," *IEEE Transactions on Biomedical Engineering*, vol. 56, no. 2, pp. 320–327, 2009.

[10] S. O. Aase, T. Eftestol, J. Husoy, K. Sunde, and P. A. Steen, "CPR artifact removal from human ECG using optimal multichannel filtering," *IEEE Transactions on Biomedical Engineering*, vol. 47, no. 11, pp. 1440–1449, 2000.

[11] J. Eilevstjønn, T. Eftestøl, S. O. Aase, H. Myklebust, J. H. Husøy, and P. A. Steen, "Feasibility of shock advice analysis during CPR through removal of CPR artefacts from the human ECG," *Resuscitation*, vol. 61, no. 2, pp. 131–141, 2004.

[12] J. Husoy, J. Eilevstjonn, T. Eftestol, S. O. Aase, H. Myklebust, and P. A. Steen, "Removal of cardiopulmonary resuscitation artifacts from human ECG using an efficient matching pursuit-like algorithm," *IEEE Transactions on Biomedical Engineering*, vol. 49, no. 11, pp. 1287–1298, 2002.

[13] K. Rheinberger, T. Steinberger, K. Unterkofler, M. Baubin, A. Klotz, and A. Amann, "Removal of CPR artifacts from the ventricular fibrillation ECG by adaptive regression on lagged reference signals," *IEEE Transactions on Biomedical Engineering*, vol. 55, no. 1, pp. 130–137, 2008.

[14] E. Aramendi, U. Ayala, U. Irusta, E. Alonso, T. Eftestøl, and J. Kramer-Johansen, "Suppression of the cardiopulmonary resuscitation artefacts using the instantaneous chest compression rate extracted from the thoracic impedance," *Resuscitation*, vol. 83, no. 6, pp. 692–698, 2012.

[15] U. Irusta, J. Ruiz, S. R. de Gauna, T. EftestØl, and J. Kramer-Johansen, "A least mean-square filter for the estimation of the cardiopulmonary resuscitation artifact based on the frequency of the compressions," *IEEE Transactions on Biomedical Engineering*, vol. 56, no. 4, pp. 1052–1062, 2009.

[16] Y. Gong, P. Gao, L. Wei, C. Dai, L. Zhang, and Y. Li, "An enhanced adaptive filtering method for suppressing cardiopulmonary resuscitation artifact," *IEEE Trans Biomed Eng*, vol. 64, no. 2, pp. 471–478, Feb 2017.

[17] J. Ruiz, U. Irusta, S. R. de Gauna, and T. Eftestøl, "Cardiopulmonary resuscitation artefact suppression using a kalman filter and the frequency of chest compressions as the reference signal," *Resuscitation*, vol. 81, no. 9, pp. 1087–1094, 2010.

[18] A. Amann, A. Klotz, T. Niederklapfer, A. Kupferthaler, T. Werther, M. Granegger, W. Lederer, M. Baubin, and W. Lingnau, "Reduction of CPR artifacts in the ventricular fibrillation ECG by coherent line removal," *Biomedical engineering online*, vol. 9, no. 1, p. 2, 2010.

[19] G. Zhang, T. Wu, Z. Wan, Z. Song, M. Yu, D. Wang, L. Li, F. Chen, and X. Xu, "A method to differentiate between ventricular fibrillation and asystole during chest compressions using artifact-corrupted ECG alone," *Computer Methods and Programs in Biomedicine*, vol. 141, pp. 111–117, 2017.

[20] S. R. de Gauna, J. Ruiz, U. Irusta, E. Aramendi, T. Eftestøl, and J. Kramer-Johansen, "A method to remove CPR artefacts from human ECG using only the recorded ECG," *Resuscitation*, vol. 76, no. 2, pp. 271–278, 2008.

[21] Y. Li, J. Bisera, F. Geheb, W. Tang, and M. H. Weil, "Identifying potentially shockable rhythms without interrupting cardiopulmonary resuscitation," *Critical care medicine*, vol. 36, no. 1, pp. 198–203, 2008.

[22] Y. Li, J. Bisera, M. H. Weil, and W. Tang, "An algorithm used for ventricular fibrillation detection without interrupting chest compression," *IEEE Trans Biomed Eng*, vol. 59, no. 1, pp. 78–86, Jan 2012.

[23] H. Kwok, J. Coult, M. Drton, T. D. Rea, and L. Sherman, "Adaptive rhythm sequencing: A method for dynamic rhythm classification during cpr," *Resuscitation*, vol. 91, pp. 26–31, Jun 2015.

[24] V. Krasteva, I. Jekova, I. Dotsinsky, and J.-P. Didon, "Shock advisory system for heart rhythm analysis during cardiopulmonary resuscitation using a single ECG input of automated external defibrillators," *Annals of biomedical engineering*, vol. 38, no. 4, pp. 1326–1336, 2010.

[25] U. Ayala, U. Irusta, J. Ruiz, T. Eftestøl, J. Kramer-Johansen, F. Alonso-Atienza, E. Alonso, and D. González-Otero, "A reliable method for rhythm analysis during cardiopulmonary resuscitation," *BioMed research international*, vol. 2014, 2014.

[26] S. Rubertsson, E. Lindgren, D. Smekal, O. Östlund, J. Silfverstolpe, R. A. Lichtveld, R. Boomars, B. Ahlstedt, G. Skoog, R. Kastberg, D. Halliwell, M. Box, J. Herlitz, and R. Karlsten, "Mechanical chest compressions and simultaneous defibrillation vs conventional cardiopulmonary resuscitation in out-of-hospital cardiac arrest: the LINC randomized trial," *JAMA*, vol. 311, no. 1, pp. 53–61, Jan 2014.

[27] L. Wik, J.-A. Olsen, D. Persse, F. Sterz, M. Lozano, Jr, M. A. Brouwer, M. Westfall, C. M. Souders, R. Malzer, P. M. van Grunsven, D. T. Travis, A. Whitehead, U. R. Herken, and E. B. Lerner, "Manual vs. integrated automatic load-distributing band CPR with equal survival after out of hospital cardiac arrest. the randomized CIRC trial," *Resuscitation*, vol. 85, no. 6, pp. 741–8, Jun 2014.

[28] M. E. H. Ong, K. E. Mackey, Z. C. Zhang, H. Tanaka, M. H.-M. Ma, R. Swor, and S. Do Shin, "Mechanical CPR devices compared to manual CPR during out-of-hospital cardiac arrest and ambulance transport: a systematic review," *Scandinavian journal of trauma, resuscitation and emergency medicine*, vol. 20, no. 1, p. 39, 2012.

[29] G. Putzer, P. Braun, A. Zimmermann, F. Pedross, G. Strapazzon, H. Brugger, and P. Paal, "LUCAS compared to manual cardiopulmonary resuscitation is more effective during helicopter rescue. A prospective, randomized, cross-over manikin study," *The American journal of emergency medicine*, vol. 31, no. 2, pp. 384–389, 2013.

[30] A. I. Larsen, Å. S. Hjørnevik, C. L. Ellingsen, and D. W. Nilsen, "Cardiac arrest with continuous mechanical chest compression during percutaneous coronary intervention: a report on the use of the LUCAS device," *Resuscitation*, vol. 75, no. 3, pp. 454–459, 2007.

[31] K. Sunde, L. Wik, and P. A. Steen, "Quality of mechanical, manual standard and active compression–decompression CPR on the arrest site and during transport in a manikin model," *Resuscitation*, vol. 34, no. 3, pp. 235–242, 1997.

[32] J. Soar, J. P. Nolan, B. W. Böttiger, G. D. Perkins, C. Lott, P. Carli, T. Pellis, C. Sandroni, M. B. Skrifvars, G. B. Smith *et al.*, "European resuscitation council guidelines for resuscitation 2015: Section 3. adult advanced life support," *Resuscitation*, vol. 95, pp. 100–147, 2015.

[33] J. Sullivan, R. Walker, A. Esibov, and F. Chapman, "A digital filter can effectively remove mechanical chest compression artifact," *Resuscitation*, vol. 85, p. S41, 2014.

[34] E. Aramendi, U. Irusta, U. Ayala, H. Naas, J. Kramer-Johansen, and T. Eftestøl, "Filtering mechanical chest compression artefacts from out-of-hospital cardiac arrest data," *Resuscitation*, vol. 98, pp. 41–47, 2016.

[35] *Instruction for use, Chest Compression System LUCAS^{TM} by Jolife AB/Physio-Control*, Scheelevägen 17, SE-223 70 Lund, Sweden, 2009.

[36] R. E. Kerber, L. B. Becker, J. D. Bourland, R. O. Cummins, A. P. Hallstrom, M. B. Michos, G. Nichol, J. P. Ornato, W. H. Thies, R. D. White *et al.*, "Automatic external defibrillators for public access defibrillation: recommendations for specifying and reporting arrhythmia analysis algorithm performance, incorporating new waveforms, and enhancing safety," *Circulation*, vol. 95, no. 6, pp. 1677–1682, 1997.

[37] R. W. C. G. R. Wijshoff, A. M. T. M. van Asten, W. H. Peeters, R. Bezemer, G. J. Noordergraaf, M. Mischi, and R. M. Aarts, "Photoplethysmography-based algorithm for detection of cardiogenic output during cardiopulmonary resuscitation," *IEEE Trans Biomed Eng*, vol. 62, no. 3, pp. 909–21, Mar 2015.

[38] P. Sysel and P. Rajmic, "Goertzel algorithm generalized to non-integer multiples of fundamental frequency," *EURASIP Journal on Advances in Signal Processing*, vol. 2012, no. 1, p. 56, 2012.

[39] Y. Xiao, L. Ma, and R. K. Ward, "Fast rls fourier analyzers capable of accommodating frequency mismatch," *Signal Processing*, vol. 87, no. 9, pp. 2197–2212, 2007.

[40] I. Isasi, U. Irusta, E. Aramendi, U. Ayala, E. Alonso, J. Kramer-Johansen, and T. Eftestøl, "Removing piston-driven mechanical chest compression artefacts from the ecg," in *Computing in Cardiology*, vol. 44, 2017.

[41] U. Irusta Zarandona, "New signal processing algorithms for automated external defibrillators," Ph.D. dissertation, 2010. [Online]. Available: http://hdl.handle.net/10810/7990

[42] U. Irusta, J. Ruiz, E. Aramendi, S. Ruiz de Gauna, U. Ayala, and E. Alonso, "A high-temporal resolution algorithm to discriminate shockable from nonshockable rhythms in adults and children," *Resuscitation*, vol. 83, no. 9, pp. 1090–7, Sep 2012.

[43] U. Irusta and J. Ruiz, "An algorithm to discriminate supraventricular from ventricular tachycardia in automated external defibrillators valid for adult and paediatric patients." *Resuscitation*, vol. 80, pp. 1229–1233, Nov. 2009.

[44] C. Figuera, U. Irusta, E. Morgado, E. Aramendi, U. Ayala, L. Wik, J. Kramer-Johansen, T. Eftestl, and F. Alonso-Atienza, "Machine learning techniques for the detection of shockable rhythms in automated external defibrillators." *PloS one*, vol. 11, p. e0159654, 2016.

[45] A. B. Rad, T. Eftestol, K. Engan, U. Irusta, J. T. Kvaloy, J. Kramer-Johansen, L. Wik, and A. K. Katsaggelos, "ECG-based classification of resuscitation cardiac rhythms for retrospective data analysis," *IEEE Transactions on Biomedical Engineering*, 2017.

[46] P. Govindarajan, L. Lin, A. Landman, J. T. McMullan, B. F. McNally, A. J. Crouch, and C. Sasson, "Practice variability among the ems systems participating in cardiac arrest registry to enhance survival (cares)," *Resuscitation*, vol. 83, no. 1, pp. 76–80, 2012.

[47] U. Ayala, J. Eilevstjnn, U. Irusta, T. Eftestl, E. Alonso, and D. Gonzalez, "Are dual-channel methods as accurate as multi-channel methods to suppress the cpr artifact?" in *Proc. Computing in Cardiology*, Sep. 2011, pp. 509–512.

[48] E. Aramendi, S. R. de Gauna, U. Irusta, J. Ruiz, M. F. Arcocha, and J. M. Ormaetxe, "Detection of ventricular fibrillation in the presence of cardiopulmonary resuscitation artefacts," *Resuscitation*, vol. 72, no. 1, pp. 115–123, 2007.